J. Chem. Sci. (2020)132:69
https://doi.org/10.1007/s12039-020-01777-2
© Indian Academy of Sciences

REGULAR ARTICLE

Sensitive determination of kojic acid in tomato sauces using Ni–Fe layered double hydroxide synthesized through Fe-MIL-88 metal-organic framework templated route

DHARMENDRA KUMAR YADAV[a], VELLAICHAMY GANESAN[a,*], RUPALI GUPTA[a], MAMTA YADAV[a] and PANKAJ KUMAR RASTOGI[b]

[a]Department of Chemistry, Institute of Science, Banaras Hindu University, Varanasi 221 005, Uttar Pradesh, India

[b]Department of Chemistry, GLA University, Mathura, Uttar Pradesh 284 401, India

E-mail: velganesh@yahoo.com; velgan@bhu.ac.in

MS received 21 November 2019; revised 4 February 2020; accepted 8 February 2020

Abstract. A sacrificial template, Fe-MIL-88 is used to synthesize Ni–Fe layered double hydroxide (Ni–Fe LDH). The metal-organic framework (Fe-MIL-88) is synthesized from the precursors, ferric nitrate and terephthalic acid. Electrocatalytic oxidation of kojic acid (KA) is realized by Ni–Fe LDH film which is coated on a glassy carbon electrode (GC). Under the optimized conditions, amperometry measurements at the Ni–Fe LDH coated GC as a function of KA concentration demonstrates a sensitive determination of KA. The calibration curve shows two linear ranges, 1–1500 μM and 1500–4500 μM for the KA determination. Detection limit for the KA determination is estimated as 0.73 μM. The practical applicability of this method is confirmed by measuring the KA concentration present in various real samples.

Keywords. Ni–Fe LDH; Fe-MIL-88; kojic acid; amperometry; electrocatalysis; sacrificial template.

1. Introduction

Designing specific layered double hydroxides (LDHs) with tailor-made properties to suit the desired applications have drawn great attention due to their potential applications in biotechnology, energy storage, separation science, adsorbents, photochemistry, electrochemistry, etc.[1–10] Generally, LDHs are synthetic lamellar solids with metal cations (trivalent and divalent) and anions (n-valent). Their general formula can be given as $[M^{2+}_{1-y}\ M^{3+}_{y}\ (OH)_2]^{y+}\ [(A^{n-})_{y/n},\ y\ H_2O]$.[11] LDHs can be synthesized by conventional methods like ion-exchange, co-precipitation, and hydrothermal methods.[12,13] However, these methods are not efficient in controlling the morphology, surface area, and particle size of the LDHs.[13] Due to this limitation, the application of LDHs as catalysts, adsorbents, and electrode modifiers are limited.[14] To overcome this drawback and to explore their electrocatalytic properties, a new Ni–Fe LDH which is synthesized using a template based on Fe(III) metal-organic framework (MOF) is reported. This new Ni–Fe LDH is envisaged to exhibit high surface area, high adsorption capacity, and enhanced catalytic activity. Kojic acid (KA), otherwise known as 5-hydroxy-2-(hydroxymethyl)-4-pyrone (based on IUPAC recommended nomenclature) is globally used as an antioxidant, food additive, or preservative.[15–17] KA is generally extracted from the fungal genus Aspergillus.[15–17] However, its safety assessment is controversial due to carcinogenicity, teratogenicity, and embryotoxicity.[18,19] Therefore, monitoring of KA concentration levels is very important due to its human health issues, food safety, and quality control aspects.[18,20] Real-time monitoring/determination of KA can be achieved by several techniques like ion-pair liquid chromatography, capillary electrophoresis, fluorimetry and electrochemical methods.[21–24] Among these methods, the electrochemical method generally receives great attention since it can offer a sensitive,

*For correspondence

Electronic supplementary material: The online version of this article (https://doi.org/10.1007/s12039-020-01777-2) contains supplementary material, which is available to authorized users.

Published online: 28 May 2020

selective, simple, and cost-effective route for many target analyte determinations.[25–27] Accordingly, in this work, we report an electrochemical method for the quantitative assay of KA using a MOF templated Ni–Fe LDH for the first time.

2. Experimental

2.1 *Materials and reagents*

N,*N*-dimethylformamide (DMF), poly(vinyl alcohol), nickel acetate tetrahydrate and benzene-1,4-dicarboxylic acid were supplied by S.D. Fine Chemicals, India. Potassium ferrocyanide, potassium ferricyanide, potassium chloride, K_2HPO_4, KH_2PO_4, and ferric nitrate were procured from Qualigens, India. Kojic acid (KA) was obtained from Himedia, India. Stock solutions of K_2HPO_4 and KH_2PO_4 were used for the preparation of 0.1 M pH 7.0 phosphate buffer. Triple distilled water was used for electrochemical experiments.

Fe-MIL-88 and Ni–Fe LDH were synthesized hydrothermally as described before in our previous publication.[14] The synthesis of Fe-MIL-88 is carried out using a mixture of benzene-1,4-dicarboxylic acid and ferric nitrate in DMF-ethanol-water mixture. The mixture was ultra-sonicated, stirred, refluxed at 80 °C under the stirring condition for 12 h, and finally subjected to centrifugation (8000 rpm). The obtained precipitate (Fe-MIL-88) was washed multiple times with a mixture of ethanol-water and then dried for 24 h at 60 °C. Synthesis of Ni–Fe LDH was accomplished by mixing the required amounts of Fe-MIL-88 (0.02 g) and nickel acetate tetrahydrate (0.2 M) in DMF. This mixture was then subjected to ultra-sonication and refluxed with stirring at 85 °C for 4 h. Further, DMF and water were added to the mixture and refluxed at 120 °C for an additional 12 h. Then the mixture was cooled to room temperature and centrifuged to get the Ni–Fe LDH. The formed Ni–Fe LDH was filtered, washed with a large amount of water, and dried for 5 h at 120 °C.[14,28]

2.2 *Apparatus*

X-ray diffraction (XRD) patterns (BRUKER D8 X-ray diffractometer with Cu Kα line (0.159 nm), X-ray photoelectron spectroscopy (XPS, AMICUS spectrometer, UK), scanning electron microscopy (SEM) (SEM VEGA 3 TESCAN at 30 kV) and transmission electron microscopy (TEM) (TECNAI 20 G2 FEI microscope; 120 kV) analyses were carried out for the characterization of the materials. Cyclic voltammetry, amperometry, and chronoamperometry measurements were accomplished with CHI-660C electrochemical workstation (CH Instruments, USA). Glassy carbon (GC) or modified GC, platinum wire and saturated calomel electrode *i.e.* $Hg/Hg_2Cl_2/KCl$(sat.) were used as working, counter, and reference electrodes, respectively. GC electrode surface is modified either with Fe-MIL-88 or Ni–Fe LDH. The colloid of the respective materials (0.1 wt%) with poly(vinyl alcohol) (0.01 wt%) were prepared and typically 20 µL of the colloid was drop coated and dried for 4 h to get the modified GC electrodes. The modified electrodes were represented as GC/Fe-MIL-88 or GC/Ni–Fe LDH. It should be noted that the present work reports the construction of Fe-MIL-88 or Ni–Fe LDH film prepared on GC electrodes. However, carbon paste electrodes (CPEs) using the Fe-MIL-88 or Ni–Fe LDH materials were already constructed, characterized, and demonstrated for the efficient water oxidation in alkaline medium.[14]

3. Results and Discussion

3.1 *Characterization of Ni–Fe LDH*

Detailed characterization of Fe-MIL-88 and Ni–Fe LDH were elaborately discussed based on the results of TEM, XRD patterns, and XPS in our earlier study.[14] The powder XRD data are provided in supplementary information, Table S1 (Supplementary Information).[14] The powder XRD patterns of Fe-MIL-88 show peaks at the 2θ values of 8.9°, 16.2°, and 17.3° which can be attributed to (002), (103), and (200) planes of Fe-MIL-88, respectively (Table S1, Supplementary Information).[14] Ni–Fe LDH shows additional peaks at the 2θ values 11.7°, 23.7°, 34.8°, 39.5°, 59.5°, and 61.0° which are ascribed to various crystal planes of Ni–Fe LDH, respectively (Table S1, Supplementary Information).[14] Spindle shaped morphology of Fe-MIL-88 and porous layered structure of Ni–Fe LDH are revealed from the SEM and TEM analyzes (Figure S1, Supplementary Information).[14] The XPS of Fe $2p_{1/2}$ (726.1 eV) and Fe $2p_{3/2}$ (712.6 eV) in both Fe-MIL-88 and Ni–Fe LDH materials confirm the +3 oxidation state of Fe (Table S2, Supplementary Information,).[14] Similarly, the XPS of Ni $2p_{3/2}$ (856.7 and 851.8 eV) and Ni $2p_{1/2}$ (872.3 eV) in Ni–Fe LDH confirm the presence of +2 and +3 oxidation states of Ni (Table S2, Supplementary Information).[14] The FT-IR spectrum[14] of Ni–Fe LDH displays peaks at 1107 and

876 cm^{-1} which can be corroborated to the deformation of –OH. A peak around 876 cm^{-1} is also observed[14] owing to the out of plane deformation of carbonate species present in the Ni–Fe LDH.[14] Electrochemical impedance analyzes of CPEs based on these materials were already reported.[14] In the present study, electrochemical impedance analyzes are carried out with the Fe-MIL-88 and Ni–Fe LDH film modified electrodes to understand the electron transfer activities within the film. Aqueous ferrocyanide/ferricyanide redox couple (10.0 mM $K_3[Fe(CN)_6]$ and 10.0 mM $K_2[Fe(CN)_6]$) is used as a probe and the analyzes are carried out with 0.1 M KCl by applying 0.2 V at GC/Fe-MIL-88 and GC/Ni–Fe LDH electrodes (Figure 1). The cyclic voltammetry (CV) responses of the probe at GC/Fe-MIL-88 and GC/Ni–Fe LDH are also recorded (inset (i) of Figure 1). Both GC/Fe-MIL-88 and GC/Ni–Fe LDH electrodes show redox peaks corresponding to $[Fe(CN)_6]^{3-/4-}$ redox process. GC/Fe-MIL-88 shows a slightly low peak current with a ΔEp value of 140 mV while the GC/Ni–Fe LDH electrode shows a high peak current with a ΔEp value of 180 mV. These results suggest that the electrical conductivity inside the Ni–Fe LDH film is greater than the Fe-MIL-88 film (based on high current obtained at GC/Ni–Fe LDH electrode). Nyquist plots demonstrate that two different physicochemical processes take place at the electrode-solution interface which may be referred as charge transfer phenomena inside the sheets of Ni–Fe LDH or Fe-MIL-88 and a heterogeneous electron transfer process between the modified electrode and the electrolyte solution.[29] A suitable Randle's equivalent circuit is identified (inset (ii) of Figure 1) which relies on the experimentally observed data. As per the Randle's equivalent circuit, it possesses three resistance components, the resistance of electrolyte (R_1), charge transfer resistance (R_{ct}), and resistive part of the mass transfer (R_p), mass transfer resistance (Z_d), the capacitance of the film (C_{dl}) and two constant phase elements (Q_1 and Q_2). The Ni–Fe LDH displays a semicircle with a lesser diameter than the Fe-MIL-88 indicating lower R_{ct} value than that of the Fe-MIL-88. This low R_{ct} leads to a fast electron transfer process at GC/Ni–Fe LDH electrode. Presence of Ni^{3+} in the Ni–Fe LDH and/or the broad interlayer space of Ni–Fe LDH may cause increased conductivity within the film.[14,30]

3.2 *Electrochemical determination of KA*

Cyclic voltammograms are recorded in phosphate buffer (0.1 M, pH 7.0) with and without KA (100 μM) using GC, GC/Fe-MIL-88, and GC/Ni–Fe LDH electrodes (Figure 2). No significant redox behavior is noticed in the absence of KA at all the electrodes (inset of Figure 2). However, in the presence of KA, a well-defined voltammetric peak is observed due to the efficient electro-oxidation of KA at all the three electrodes (Figure 2a′–2c′). At bare GC and GC/Fe-MIL-88 electrodes (Figure 2a′ and 2b′), KA is oxidized at 0.79 V with a low current. At GC/Ni–Fe LDH

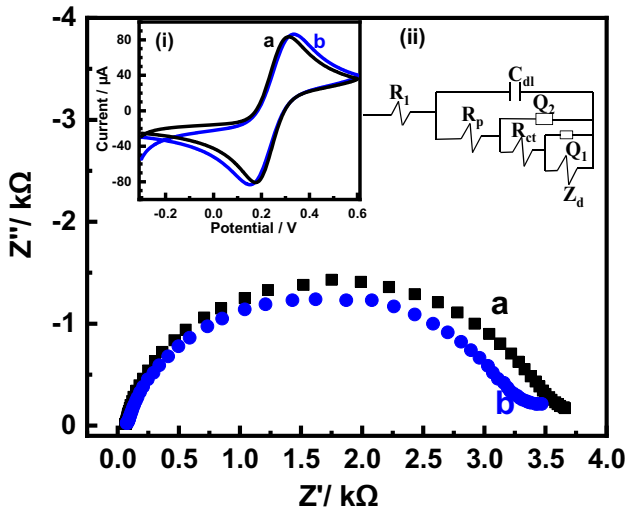

Figure 1. Nyquist plots for the GC/Fe-MIL-88 (**a**) and GC/Ni–Fe LDH (**b**). Inset (i) represents the cyclic voltammograms of GC/Fe-MIL-88 (**a**) and GC/Ni–Fe LDH (**b**) in a mixture of 10.0 mM $K_3[Fe(CN)_6]$, 10.0 mM $K_2[Fe(CN)_6]$, and 0.1 M KCl. Inset (ii) shows the suitable Randle's equivalent circuit.

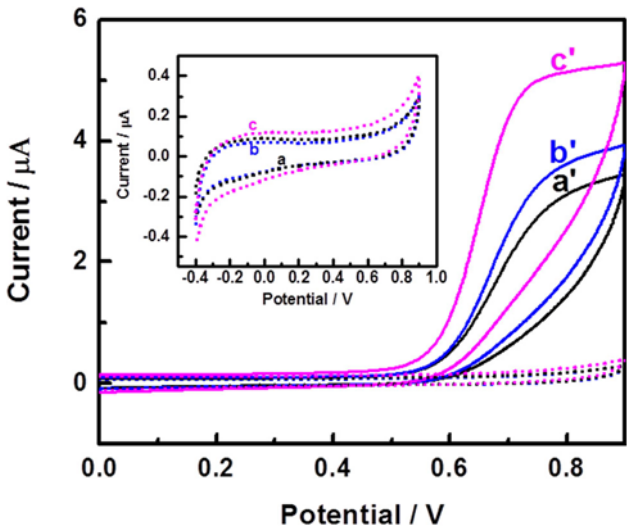

Figure 2. Cyclic voltammograms of bare GC (**a** and **a′**), GC/Fe-MIL-88 (**b** and **b′**), and GC/Ni–Fe LDH (**c** and **c′**) in 0.1 M phosphate buffer (pH 7.0) in the presence (**a′**, **b′**, and **c′**) and absence (**a**, **b**, and **c**) of 100 μM KA at 20 mV s^{-1} scan rate.

electrode, KA is oxidized at 0.75 V with a high current. Thus, GC/Ni–Fe LDH exhibits low oxidation peak potential and high peak current for KA electrooxidation in comparison to bare GC and GC/Fe-MIL-88 electrodes which indicate the efficient electrocatalytic activity of GC/Ni–Fe LDH. This electrocatalytic activity may be due to the involvement of Ni^{3+} present in Ni–Fe LDH.

Efficient electrocatalytic oxidation of KA at the GC/Ni–Fe LDH electrode may lead to a sensitive determination of KA which can be verified by amperometry using the GC/Ni–Fe LDH electrode. The amperometry responses arising from successive additions of KA are recorded ($E_{applied}$: 0.6 V) in 0.1 M pH 7.0 phosphate buffer (Figure 3A). The calibration curve from the amperometry responses is drawn for KA determination which shows two linear responses (Figure 3B). The first linear response is spread over the KA concentration range from 1.0 μM to 1.5 mM and the next linear range is observed from 1.5 to 4.5 mM. The sensitivity and detection limit for the KA determination are found to be 0.032 μA μM^{-1} cm^{-2} and 0.73 μM, respectively. On increasing the concentration above 1.5 mM of KA, the rate of the electrocatalytic reaction may become slow due to saturation of the active catalytic sites[31] which results in a decreased sensitivity of the second linear region of the calibration plot. The sensitivity of the present method is comparable to many of the recently reported methods.[15,17,32–37] Although certain methods show slightly high sensitivity, they exhibit a narrow linear calibration range.[15,35] Thus, the present method demonstrates higher sensitivity and wider linear calibration range than the previous methods for the determination of KA.[15,35,37] Therefore, the present method is comparable or superior with previously reported methods for KA determination as shown in Table 1. [32–37]

3.3 *Chronoamperometry of KA oxidation*

The oxidation of KA is further studied by chronoamperometry to understand the kinetics of the GC/Ni–Fe LDH electrode process and shown in Figure 4. From the slope of the plot shown in the inset of Figure 4, the value of the catalytic rate constant (K_C) is calculated to be 1.96×10^5 M^{-1} s^{-1} using equation 1.[17]

$$\frac{I_{cat}}{I_L} = \sqrt{K_C C_b \pi t} \tag{1}$$

where I_{cat} (catalytic current) is the anodic oxidation currents measured in the presence of different concentrations of KA and I_L (limiting current) is the current obtained in the absence of KA. C_b is the bulk concentration of KA and t is the time. The value of K_C for KA oxidation agrees practically with other reported values.[17]

Based on the above studies and in line with the literature,[38] the mechanism of electrocatalytic oxidation of KA by the Ni–Fe LDH may be postulated as displayed in equations 2–4.

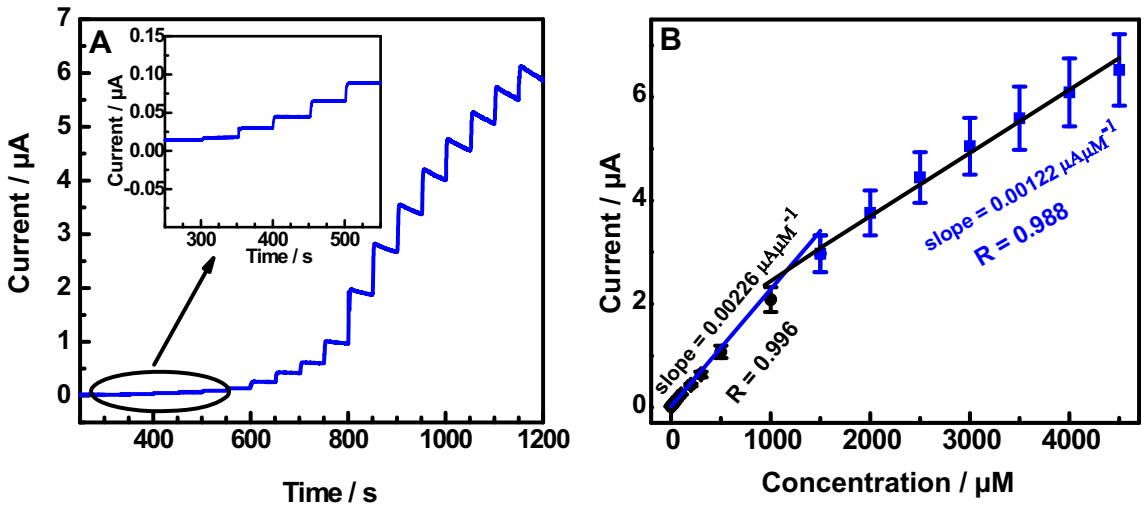

Figure 3. (**A**) Amperometric response of GC/Ni–Fe LDH with successive additions of KA (1, 5, 10, 20, 30, 50, 100, 200, 300, 500, 1000, 1500, 2000, 2500, 3000, 3500, 4000 and 4500 μM) into 0.1 M phosphate buffer. Expanded view from 1 to 30 μM additions of KA is shown in the inset. (**B**) Calibration curve showing the two linear ranges (1–1500 μM and 1500–4500 μM) for KA determination with error bars.

Table 1. An assessment of key analytical factors for the electrochemical KA determination.

Material and electrode	Technique	Sensitivity ($\mu A\ \mu M^{-1}$)	Linear range (μM)	Detection limit (μM)	References
Hollow CuO/Fe_2O_3-Chi/GC	Amperometry	0.0302	0.2–674	0.08	32
CNT-SPCE	DPV	0.0016	20–5000	16	15
Ionic liquid and V_2O_5/NPs/GC	SWV	0.1022	0.08–500	0.02	17
MWCNT/ARS film-modified GC	Amperometry	0.055	0.4–60	0.1	33
Graphene-Pt nanocomposite	DPV	0.139	0.2–1000	0.2	34
Poly(glutamic acid)/GC	CV	–	8.0–660	0.8	35
EPPG/GC	LSV	0.73	0.75–15	0.23	36
Reduced graphene sheet	LSV	0.0429	10–140	–	37
GC/Ni–Fe LDH	Amperometry	0.032	1–1500, 1500–4500	0.77	This work

Chi chitosan, *GC* glassy carbon electrode, *MWCNT* multi-walled carbon nanotubes, *SPCE* screen-printed carbon electrode, *NPs* nanoparticles, *ARS* alizarin red S, *EPPG* edge plane pyrolytic graphite, *DPV* differential pulse voltammetry, *SWV* square wave voltammetry, *CV* cyclic voltammetry, *LSV* linear sweep voltammetry.

$$\mathrm{Ni(II)-Fe\ LDH} \rightleftarrows \mathrm{Ni(III)-Fe\ LDH} + e^- \quad (2)$$

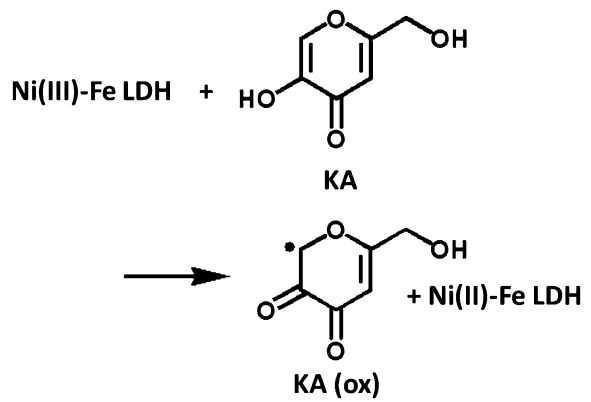

(3)

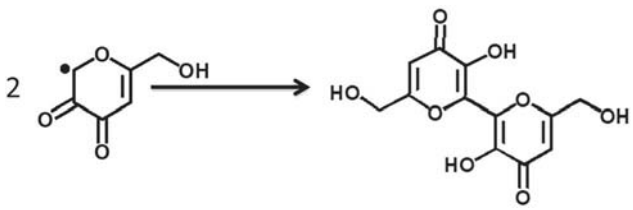

(4)

In the given mechanism, Ni(II)-Fe LDH is electrochemically oxidized to Ni(III)-Fe LDH and KA is chemically oxidized to $KA_{(ox)}$ by the electrogenerated Ni(III)-Fe LDH involving one electron and one proton. The oxidized KA ($KA_{(ox)}$) undergoes further reaction to produce 6,6′-bis(5-hydroxy-2-(hydroxymethyl)-4H-pyran-4-one as the final product (equation 4).[39]

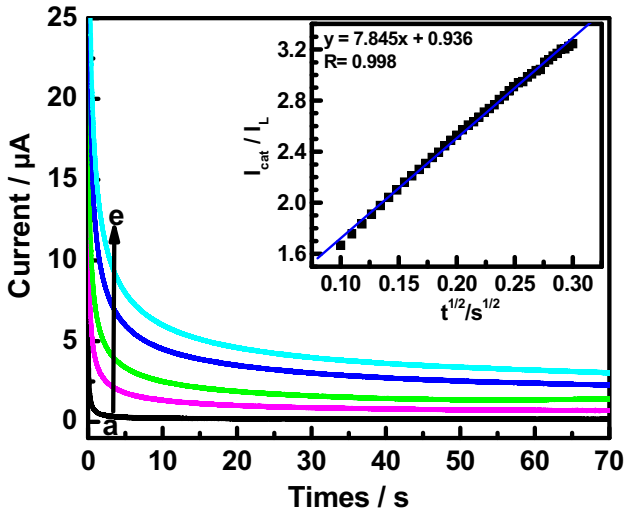

Figure 4. Chronoamperograms of GC/Ni–Fe LDH in 0.1 M phosphate buffer (pH 7.0) with varying concentrations of KA (**a**–**e**; 0, 100.0, 200.0, 400.0 and 600.0 μM, respectively). Inset shows the I_{cat}/I_L for 100 μM of KA.

3.4 *Reproducibility, stability, and interference studies*

The reproducibility of the GC/Ni–Fe LDH electrode is analyzed by determining 100 μM KA three times. The relative standard deviation for the three determinations is calculated as 5.6% which reveals an acceptable reproducibility. The storage stability of GC/Ni–Fe LDH is tested by keeping the electrode under the room temperature condition for 7 days and comparing the CV response of the first and seventh days for the determination of 100 μM KA. On the seventh day, GC/Ni–Fe LDH exhibits 95.0% of the initial signal

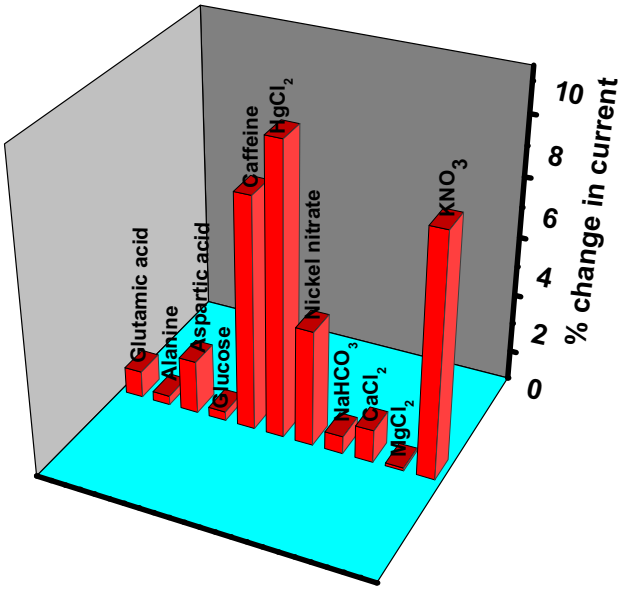

Figure 5. Percentage signal alteration for the determination of KA in the presence of possible interferents at GC/ Ni–Fe LDH electrode in 0.1 M phosphate buffer (pH 7.0) at 20 mV s^{-1}.

(first-day current response), which reveals reasonable stability of the GC/ Ni–Fe LDH.

The selectivity of the GC/Ni–Fe LDH electrode towards the determination of 100 μM KA is analyzed in the presence of several possible interferents (Figure 5). The influence of possible coexisting common salts (2.0 mM of each salt like KNO_3, $MgCl_2$, $CaCl_2$, $NaHCO_3$, $Ni(NO_3)_2$ and $HgCl_2$) and biomolecules (1.0 mM of each compound like caffeine, glucose, aspartic acid, alanine, and glutamic acid) in the determination of KA is investigated (Figure 5).[34] Many of the added interferents exhibit negligible influence (less than ±5%) during the determination of 100 μM KA. Few interferents show a signal change slightly higher than ± 5%, however, less than 10% indicating the high selectivity of this method. Thus, GC/Ni–Fe LDH can be used for the reliable quantitative determination of KA.

Table 2. Determination of KA present in different brands of tomato sauce samples.

Sample (brand)	Added (μM)	Measured (μM)	Recovery (%)	RSD (n = 3, %)
Sauce A (Tombo)	–	2	–	6.2
	100	108	106	0.8
Sauce B (Kissan)	–	2	–	9.7
	100	90	88	4.9
Sauce C (Maggi pichkoo)	–	1	–	5.8
	100	87	86	3.9

3.5 *Determination of KA in different tomato sauces*

The realistic use of the sensor is established by analyzing KA present in the commercially available tomato sauces, A (Tombo), B (Kissan), and C (Maggi pichkoo). The samples (sauce A, B, and C) were diluted with water and analyzed using GC/Ni–Fe LDH electrode in 0.1 M phosphate buffer. Tomato sauce may contain Fe^{3+}, ascorbic acid, oxalic acid, gallotannic acid, etc. However, they are estimated to be present in a very small amount. Therefore, these interferents cannot affect the response due to KA. The amperometry current response is measured for all three sauces (alone and also spiked with standard KA). The results are illustrated in Table 2. Reasonable recovery justifies the use of the GC/Ni–Fe LDH electrode for the estimation of KA in real samples. The results are comparable with the previously reported methods.[21,40]

4. Conclusions

Fe-MIL-88 is used as a template to synthesize Ni–Fe LDH. Based on the efficient electrocatalytic oxidation of KA by Ni–Fe LDH, the quantitative determination of KA is realized. The performance characteristics of the GC/Ni–Fe LDH electrode with those of the earlier reports revealed that the proposed sensor exhibits low overpotential for the oxidation of KA. The quantitative determination of KA is not affected even in the presence of many possible interfering compounds. It could be useful for the direct determination of KA in real samples without any pretreatments.

Supplementary information (SI)

Tables S1–S2 and Figure S1 are available at www.ias.ac.in/chemsci.

Acknowledgements

Generous financial support from DST-ASEAN (IMRC/AISTDF/R&D/P-16/2018) and DST (SR/NM/NS-2012/2013(G)), New Delhi is gratefully acknowledged. DKY acknowledges UGC, New Delhi for Senior Research Fellowship.

References

1. Chen H, Mousty C, Cosnier S, Silveira C, Moura J J G and Almeida M G 2007 Highly sensitive nitrite

biosensor based on the electrical wiring of nitrite reductase by [ZnCr-AQS] LDH *Electrochem. Commun.* **9** 2240
2. Kameyama T, Okazaki K I, Takagi K and Torimoto T 2009 Stacked-structure-dependent photoelectrochemical properties of CdS nanoparticle/layered double hydroxide (LDH) nanosheet multilayer films prepared by layer-by-layer accumulation *Phys. Chem. Chem. Phys.* **11** 5369
3. Zhao Y, He S, Wei M, Evans D G and Duan X 2010 Hierarchical films of layered double hydroxides by using a sol-gel process and their high adaptability in water treatment *Chem. Commun.* **46** 3031
4. Radha A, Kamath P V and Shivakumar C 2007 Conservation of order, disorder and crystallinity during anion-exchange reactions among layered double hydroxides (LDHs) of Zn with Al *J. Phys. Chem. B* **111** 3411
5. Dixit M, Jayashree R S, Kamath P V, Shukla A K, Kumar V G and Munichandraiah N 1999 Electrochemically impregnated aluminum stabilized alpha nickel hydroxide batteries *Electrochem. Solid State Lett.* **2** 170
6. Zadeh H A, Kohansal S and Sadeghi G H 2011 Selective solid-phase extraction and spectrofluorometric determination of salicylic acid in pharmaceutical and biological samples *Talanta* **84** 368
7. Shan D, Wang Y N, Zhu M J, Xue H G, Cosnier S and Wang C Y 2009 Development of a high analytical performance-xanthine biosensor based on layered double hydroxides modified-electrode and investigation of the inhibitory effect by allopurinol *Biosens. Bioelectron.* **24** 1171
8. Qiu J B 1995 Anionic clay modified electrodes: electrochemical activity of nickel(II) sites in layered double hydroxide films. *J. Electroanal. Chem.* **395** 159
9. Reichle W T 1986 Synthesis of anionic clay minerals (mixed metal hydroxides, hydrotalcite) *Solid State Ion.* **22** 135
10. Yao L, Wei D, Yan D and Hu C 2015, ZnCr Layered double hydroxide (LDH) nanosheets assisted formation of hierarchical flower-like CdZnS@LDH microstructures with improved visible-light-Driven H_2 production *Chem. Asian J.* **10** 630
11. Tonelli D, Scavetta E and Giorgetti M 2013 Layered-double-hydroxide-modified electrodes: electroanalytical applications *Anal. Bioanal. Chem.* **405** 603
12. Wang Q and O'Hare D 2012 Recent advances in the synthesis and application of layered double hydroxide (LDH) nanosheets *Chem. Rev.* **112** 4124
13. Jiang Z, Li Z, Qin Z, Sun H, Jiao X and Chen D 2013 LDH nanocages synthesized with MOF templates and their high performance as supercapacitors *Nanoscale* **5** 11770
14. Yadav D K, Ganesan V, Sonkar P K and Gupta R 2017 Templated synthesis of nickel@iron layered double hydroxide for enhanced electrocatalytic water oxidation: towards the development of non-precious-metal catalysts *ChemElectroChem* **4** 3134
15. Buleandra M, Rabinca A A, Tache F, Moldovan Z, Stamatin I, Mihailciuc C and Ciucu A A 2017 Rapid voltammetric detection of kojic acid at a multi-walled carbon nanotubes screen-printed electrode *Sens. Actuat. B-Chem.* **241** 406
16. Ma X and Chao M 2014 Study on the electrochemical properties of kojic acid at a poly(glutamic acid)-modified glassy carbon electrode and its analytical application *Food Anal. Methods* **7** 1458
17. Sheikhshoaie M, Sheikhshoaie I and Ranjbar M 2017 Analysis of kojic acid in food samples uses an amplified electrochemical sensor employing V_2O_5 nanoparticle and room temperature ionic liquid *J. Mol. Liq.* **231** 597
18. Gao Z, Su R, Qi W, Wang L and He Z 2014 Copper nanocluster-based fluorescent sensors for sensitive and selective detection of kojic acid in food stuff *Sens. Actuat. B-Chem.* **195** 359
19. Chusiri Y, Wongpoomchai R, Kakehashi A, Wei M, Wanibuchi H, Vinitketkumnuan U and Fukushima S 2011 Non-genotoxic mode of action and possible threshold for hepatocarcinogenicity of kojic acid in F344 rats *Food Chem. Toxicol.* **49** 471
20. Blumenthal C Z 2004 Production of toxic metabolites in *Aspergillus niger*, *Aspergillus oryzae*, and *Trichoderma reesei*: justification of mycotoxin testing in food grade enzyme preparations derived from the three fungi *Toxicol. Pharmacol.* **39** 214
21. Shih Y 2001 Simultaneous determination of magnesium L-ascorbyl-2-phosphate and kojic acid cosmetic bleaching products by using a microbore column and ion-pair liquid chromatography *J. AOAC Int.* **84** 1045
22. Lin Y H, Yang Y H and Wu S M 2007 Experimental design and capillary electrophoresis for simultaneous analysis of arbutin, kojic acid and hydroquinone in cosmetics *J. Pharm. Biomed. Anal.* **44** 279
23. Song P, Xiang Y, Xing H, Zhou Z, Tong A and Lu Y 2012 Label-free catalytic and molecular beacon containing an abasic site for sensitive fluorescent detection of small inorganic and organic molecules *Anal. Chem.* **84** 2916
24. Vachalkova A, Bransova J, Brtko J, Uher M and Novotny L 1996 Polarographic behavior of kojic acid and its derivatives, determination of potential carcinogenicity and correlation of these properties with their other attributes *Neoplasma* **43** 265
25. Ziyatdinova G K, Budnikov G K and Pogoreltsev V I 2004 Electrochemical determination of lipoic acid *J. Anal. Chem.* **59** 324
26. Yashin Y I and Yashin A Y 2004 Analysis of food products and beverages using high-performance liquid chromatography and ion chromatography with electrochemical detectors *J. Anal. Chem.* **59** 1237
27. Mohammadizadeh N, Mohammadi S Z and Kaykhaii M 2018 Carbon paste electrode modified with ZrO_2 nanoparticles and ionic liquid for sensing of dopamine in the presence of uric acid *J. Anal. Chem.* **73** 685
28. Wu Y, Luo H and Wang H 2014 Synthesis of iron(III)-based metal–organic framework/graphene oxide composites with increased photocatalytic performance for dye degradation *RSC Adv.* **4** 40435
29. Shi S, Fang Z and Ni J 2005 Electrochemical impedance spectroscopy of marmatite-carbon paste electrode in the presence and absence of *Acidithiobacillus ferrooxidans* *Electrochem. Commun.* **7** 1177

30. Li B Y, Hasin P and Wu Y 2010 $Ni_xCo_{3-x}O_4$ nanowire arrays for electrocatalytic oxygen evolution *Adv. Mater.* **22** 1926
31. Rastogi P K, Ganesan V and Krishnamoorthi S 2014 Palladium nanoparticles incorporated polymer-silica nanocomposite based electrochemical sensing platform for nitrobenzene detection *Electrochim. Acta* **147** 442
32. Yang Z, Yin Z and Chen F 2011 A novel kojic acid amperometric sensor based on hollow CuO/Fe_2O_3 hybrid microspheres immobilized in chitosan matrix *Electrochim. Acta* **56** 1089
33. Liu J, Zhou D, Liu X, Wu K and Wan C 2009 Determination of kojic acid based on the interface enhancement effects of carbon nanotube/alizarin red S modified electrode *Colloids Surf. B* **70** 20
34. Wang L, Qi W, Su R and He Z 2014 Sensitive and efficient electrochemical determination of kojic acid in foodstuffs based on graphene-Pt nanocomposite-modified electrode *Food Anal. Methods* **7** 109
35. Ma X and Chao M 2014 Study on the electrochemical properties of kojic acid at a poly(glutamic acid)-modified glassy carbon electrode and its analytical application *Food Anal. Methods* **7** 1458
36. Filho L C S F, Brownson D A C, Filho O F and Banks C E 2013 Exploring the origins of the apparent "electrocatalytic" oxidation of kojic acid at graphene modified electrodes *Analyst* **138** 4436
37. Wang Y, Zhang D and Wu J 2012 Electrocatalytic oxidation of kojic acid at a reduced graphene sheet modified glassy carbon electrode *J. Electroanal. Chem.* **664** 111
38. Hai B and Zou Y 2015 Carbon cloth supported NiAl-layered double hydroxides for flexible application and highly sensitive electrochemical sensors *Sens. Actuat. B-Chem*. **208** 143
39. Bastidas F, Urzua U and Vicuna R 2002 Oxidation of kojic acid catalyzed by manganese peroxidase from *Ceriporiopsis subvermispora* in the absence of hydrogen peroxide *Appl. Biochem. Biotechnol.* **101** 31
40. Yang X and Zhang H 2007 Sensitive determination of kojic acid in foodstuffs using PVP (polyvinylpyrrolidone) modified acetylene black paste electrode *Food Chem.* **102** 1223